Current Research in Food Science 10 (2025) 101040

Contents lists available at ScienceDirect

Current Research in Food Science

journal homepage: www.sciencedirect.com/journal/current-research-in-food-science

Analysis of the correlation between the distribution of microorganisms carried by *Coix* seed and fungal toxins, and the biological control of aflatoxin

Lingxia Peng [a,1], Jiahao Fang [a,1], Lijun Yang [a], Gurusamy Abirami [a], Feng Yin [a], Lietao Cai [b], Chaojun Zhang [b], Yuyang Zhao [c], Yan Jin [c], Shuifeng Zhang [d], Huadong Sheng [d], Guohong Zeng [a], Haimin Chen [a], Zongsuo Liang [a], Xiaodan Zhang [a,*]

[a] College of Life Sciences and Medicine, Zhejiang Sci-Tech University, Hangzhou, 310018, China
[b] R&D Center of Kanglaite, Hangzhou, 310018, China
[c] State Key Lab Breeding Base Dao-Di Herbs, National Resource Center Chinese Materia Medica, Beijing, China Academy of Chinese Medical Sciences, Beijing, 100700, China
[d] Zhejiang FangYuan Testing Group Co. LTD, Hangzhou, 310018, China

ARTICLE INFO

Handling Editor: Dr. Quancai Sun

Keywords:
Coix seed
Fungi
Mycotoxins
Association analysis
Coix lacryma-Jobi L

ABSTRACT

Coix seed is a valuable crop with both medicinal and edible uses, significantly impacting economic and medical sectors. However, its contamination with fungi and mycotoxins poses serious health risks when used medicinally. Thus, identifying fungi in *Coix* seed and controlling fungal toxins is crucial. This study employs high-throughput sequencing to detect fungi in *Coix* seed samples and analyze their correlation with mycotoxin content. Our findings showed no fungal infection from seed filling to maturity, but a diverse fungal community was present in mature seeds, the relative abundance of the dominant fungal phyla varied across different regions. In GZQL, YNFYA, and GD, the Ascomycota phylum dominated, and in LN and GXBS, Basidiomycota was the predominant phylum. These genera showed significant correlations with aflatoxins, zearalenone, and deoxynivalenol, indicating their potential as mycotoxin producers. Analysis revealed that Bacillus had a negative correlation with all detected mycotoxins. Antagonistic experiments demonstrated that Bacillus strains effectively inhibited aflatoxin production by *Aspergillus flavus*. This study provides essential data for preventing fungal growth and mycotoxin accumulation in *Coix* seed, ensuring its safe use in medicine and as food. These findings provide essential data for developing targeted strategies to prevent fungal growth and mycotoxin accumulation in *Coix* seed, ensuring its safe use in both medicinal and dietary applications. By enhancing our understanding of the microbial dynamics in *Coix* seed, we can improve food safety and public health outcomes, reinforcing the importance of continued research in this field.

1. Introduction

Coix lacryma-jobi L. is a vital medicinal and edible crop known for its significant economic and medical benefits (Wu et al., 2021) and is revered as the "king" of the Poaceae family. *Coix* seed is widely used in producing porridge, tea, feed, and wine (Wang et al., 2016). It is rich in polysaccharides (Jin et al., 2023; Chen et al., 2023), protein, fatty acids, and other nutrients (Wu Y& Yuan, 2010). Its use in traditional Chinese medicine has surged, especially after the COVID-19 pandemic. *Coix* seed is known for its medicinal properties, including promoting dampness, lung function, spleen and stomach health, dispelling wind and dampness, promoting water circulation, calming the mind, and reducing carbuncles (Han et al., 2017; Jiang et al., 2024).

However, *Coix* seed is prone to fungal infection during storage, transportation, and processing post-harvest, leading to the accumulation of mycotoxins (Miren et al., 2007). Mycotoxins such as aflatoxin (AFT), zearalenone (ZEN), deoxynivalenol (DON), and T-2 toxin pose significant risks to the quality and safety of traditional Chinese medicine

* Corresponding author.
E-mail address: zhangxiaodanzstu@163.com (X. Zhang).
[1] Equal contribution.

https://doi.org/10.1016/j.crfs.2025.101040
Received 2 September 2024; Received in revised form 22 March 2025; Accepted 22 March 2025
Available online 25 March 2025

(Arcella et al., 2017). These mycotoxins are highly carcinogenic, teratogenic, and can impair liver and kidney function (Pfohl-Leszkowicz and Manderville, 2007). Excessive intake of these toxins can severely harm human health and safety. Current regulations limit mycotoxins like aflatoxin and zearalenone in *Coix* seed, typically produced by *Aspergillus*, *Penicillium*, and *Fusarium* species (Chen et al., 2015). Fungal infections and mycotoxin accumulation in grains often involve multiple fungi, leading to synergistic effects and severe diseases (Liao et al., 2023), especially in animal feed applications. Therefore, strict control over fungi and mycotoxins in *Coix* seed is essential. A comprehensive understanding of its contamination is necessary to prevent and mitigate spoilage effectively.

During the autumn harvest, *Coix* seeds are typically harvested, sun-dried, and shelled to obtain dried seeds. This process directly exposes *Coix* seeds to the field environment, making them highly susceptible to fungal infections (Jin et al., 2014). Farmers and suppliers usually package dried *Coix* seeds in burlap bags and store them in their own warehouses. Some *Coix* seeds are preserved until the next planting season, increasing the risk of contamination during growth due to fungal carriage. Storage conditions, including temperature, humidity, and moisture content, are critical factors influencing fungal growth on *Coix* seeds. From a cost-saving perspective, maintaining optimal temperature and humidity and ensuring proper sealing of storage environments are challenging, leading to an increased risk of quality deterioration and fungal toxin contamination during long-term storage. Under favorable conditions, fungi proliferate on *Coix* seed samples, resulting in mold accumulation and compromising the quality and safety of the seeds. Recent studies on fungal contamination and mycotoxin levels in *Coix* seeds are limited. Previous detections have shown significant toxin accumulation, such as aflatoxin, deoxynivalenol, and zearalenone, due to fungal infection in *Coix* seed samples.

With growing concerns about health, the issue of mycotoxin contamination in traditional Chinese medicine has gained more attention. Mycotoxins not only degrade the intrinsic quality of medicinal materials but also pose potential health risks to consumers. Therefore, monitoring and controlling residual mycotoxins in Chinese medicinal materials has become a crucial research and management focus in medicinal safety. Initial collections of various *Coix* seed samples revealed no toxin accumulation during ripening, but residual toxins were present in mature samples. This study employs high-throughput sequencing to detect fungi in *Coix* seed samples from different maturity stages and eight different regions with residual mycotoxins. The objective is to explore the fungal carrying patterns and the correlation between mycotoxins and carrying fungi in *Coix* seeds. The findings aim to provide a reference for better inhibiting mycotoxin contamination in *Coix* seed and other Chinese medicinal materials, offering new directions for protecting the quality and safety of these materials.

2. Experimental materials and methods

2.1. Experimental materials

During October and November in the autumn season, fresh *Coix* seed samples were collected at different maturity stages, specifically 45, 30, 15, and 1 day(s) before harvest. Additionally, *Coix* seed samples were gathered from different regions, In the preliminary phase, we measured mycotoxins in *Coix* seeds from 37 different regions, and selected the seeds from the 8 regions with the highest mycotoxin levels, including Guizhou Xingren (GZXR), Guizhou Qinglong (GZQL), Yunnan Fuyuan (YNFY), Yunnan Qujing (YNQJ), Guangdong (GD), Liaoning (LN), Guangxi Baise (GXBS), and Yunnan Honghe (YNHH) (Fang et al., 2024).

Voucher specimens were identified and authenticated by Professor Liang Zongsuo and subsequently deposited at the Key Laboratory of Plant Secondary Metabolism, Zhejiang Sci-Tech University, China (Specimen Numbers: 20240101001 to 20240101024). *Aspergillus flavus* was obtained from Professor Hu and stored in a 50 % glycerol solution, frozen at −80 °C. *Bacillus tequilensis* and *Bacillus velezensis* (BF4 and BS2) were sourced from Professor Zeng and stored in a 50 % glycerol solution, frozen at −80 °C.

Table 1
PCR reaction system.

Reaction components	Reaction volume
Phusion Hot start flex 2X Master Mix	12.5 μL
Upstream primers	2.5 μL
Downstream primers	2.5 μL
DNA	50 ng
Add ddH_2O to	25 μL

Table 2
PCR reaction conditions.

temperature	time	cycles
98 °C	30 s	
98 °C	10 s	32
54 °C	30 s	32
72 °C	45 s	32
72 °C	10 min	
4 °C	∞	

Table 3
Primer sequence.

Amplification fragment	Primer sequence
ITS2 (Karlsson et al., 2014)	ITS1FI2 (5′-GTGARTCATCGAATCTTTG-3′) ITS2 (5′-TCCTCCGCTTATTGATATGC-3′
V3-V4 (Klindworth et al., 2013)	341F (5′-CCTACGGGNGGCWGCAG-3′) 785R (5′-GACTACHVGGGTATCTAATCC-3′)

2.2. Experimental Equipment

The biochemical incubator model SPX-150B-Z was purchased from Shanghai Boxun Industrial Co., Ltd. Medical Equipment Factory; the electronic balance model BT 25S was purchased from Sartorius Scientific Instruments (Beijing) Co., Ltd.; the hemocytometer model XB.K.25 was purchased from Shanghai Qiujing Biochemical Reagent Instruments Co., Ltd.; the high-pressure autoclave model SANYO MLS-3750 was purchased from Sanyo Electric Co., Ltd. (Japan); the multifunctional microplate reader model Synergy HTX was purchased from BioTek Instruments, USA; the biological microscope model CNCPTECB302 was purchased from Chongqing Aut Optical Instruments; the laminar flow hood model BoXun was purchased from Boxun Industrial Co., Ltd. Medical Equipment Factory.

2.3. Experimental methods

2.3.1. DNA extraction

DNA from different samples was extracted using the CTAB according to manufacturer's instructions. Nuclear-free water was used for blank. The total DNA was eluted in 50 μL of Elution buffer and stored at −80 °C until measurement in the PCR by LC-Bio Technology Co., Ltd, Hang Zhou, Zhejiang Province, China.

2.3.2. PCR amplification

ITS1FI2 and ITS2 were selected for PCR amplification, and the PCR products were confirmed by 2 % agarose gel electrophoresis. Throughout the DNA extraction process, ultrapure water was used as a negative control to exclude the possibility of false-positive PCR results. The specific PCR reaction system, PCR reaction conditions, and primer sequences are shown in the Table 1, Table 2, and Table 3 below.

2.3.3. Quantitative, purification, and sequencing of PCR products

The PCR products were purified using AMPure XT beads (Beckman Coulter Genomics, Danvers, MA, USA) and quantified using Qubit (Invitrogen, USA). The PCR products were then examined by 2 % agarose gel electrophoresis. After electrophoresis, DNA fragments were recovered and purified using the AMPure XT beads recovery kit. The quality of the purified PCR products was subsequently evaluated using an Agilent 2100 Bioanalyzer (Agilent, USA) and an Illumina (Kapa Biosciences, Woburn, MA, USA) library quantification kit. All amplicons were sequenced using Illumina NovaSeq PE250 (PE250, CA, USA) high-throughput sequencing technology. ASV feature sequences and an ASV abundance table were obtained by performing length filtering and denoising using DADA2 through QIIME2. Singleton ASVs were removed, and the ASV abundance table was annotated using the RDP and UNITE databases to determine the abundance of each taxonomic level across samples. The final relative abundance of each species was calculated based on the abundance data.

2.3.4. Aspergillus flavus strain activation

To prepare Potato Dextrose Agar (PDA) solid medium, the PDA medium was prepared and sterilized. Under sterile conditions, the medium was poured into Petri dishes and left to solidify. *Aspergillus flavus* spores, stored at −80 °C, were rapidly thawed in a 37 °C water bath. A 10 μL aliquot of the spore suspension was added to the surface of the PDA plates and evenly spread using a spreader. The plates were then incubated at 28 °C for 10 days.

2.3.5. Preparation of Aspergillus flavus spore suspension

To prepare the *Aspergillus flavus* spore suspension, 10 μL of Triton X-100 reagent was pipetted into 100 mL of ultrapure water and mixed well. The resulting mixture was sterilized in an autoclave at 121 °C for 20 min to create the spore elution reagent. After 10–14 days of incubation, the culture dish containing *Aspergillus flavus* was retrieved. In a laminar flow hood, 3–5 mL of the spore elution reagent was added to the culture dish. *Aspergillus flavus* spores were then gently scraped from the dish using a sterilized triangular glass rod. The spores and elution reagent were transferred into a centrifuge tube using a pipette. The spore solution was filtered through quartz cotton to remove impurities and mycelium, resulting in a suspension of *Aspergillus flavus* spores. The spore suspension was diluted as needed, and the spore concentration was determined using a hemocytometer under a biomicroscope. This concentration was calculated for use in subsequent experiments and dilutions.

2.3.6. Activation of antagonistic strains of Aspergillus flavus

The LB solid medium was prepared in a sterile hood and poured into Petri dishes to solidify. The BF4 and BS2 strains, taken from −80 °C, were streaked on the plates for activation. The plates were inverted and incubated at 28 °C for 24 h. After activation, the strains were inoculated into LB liquid medium and placed in a constant-temperature shaker at 37 °C and 210 rpm for growth. A specific volume of the culture was transferred to a 96-well plate, and the absorbance was measured using a microplate reader, ensuring the OD value remained around 0.6 to achieve a uniform bacterial concentration.

2.3.7. Antagonism experiment against Aspergillus flavus

The experimental groups were as follows: Group A: Water only (negative control); Group B: Water: *Aspergillus flavus* 1:1 v/v (positive control); Group C: *Bacillus tequilensis*: *Apsergillus flavus* 1:1 v/v; Group D: *Bacillus velezensis*: *Apsergillus flavus* 1:1 v/v. Total volume of suspension per group (including that for the controls) was 400 μl. *B. tequilensis* and *B. velezensis* were the antagonists. The OD value of the antagonistic bacterial culture was maintained at approximately 0.6, and the concentration of the *A. flavus* spore suspension was 5×10^6 CFU/mL. The sealed petri dishes were placed in a biochemical incubator and incubated for 7 days in the dark.

Table 4
Liquid phase gradient elution program.

Time/min	Flow rate mL/min	A/%	B/%
0	0.3	90	10
0.5	0.3	65	35
2	0.3	65	35
2.5	0.3	60	40
4	0.3	60	40
4.5	0.3	55	45
5.5	0.3	55	45
6	0.3	50	50
7	0.3	50	50
7.5	0.3	40	60
9	0.3	40	60
9.5	0.3	90	10
12	0.3	90	10

Mass Spectrometry Conditions: Mass spectrometry conditions: Ion source: Electrospray Ionization (ESI); Detection mode: Multiple Reaction Monitoring (MRM); Desolvation temperature: 450 °C; Desolvation gas flow rate: 800 L/h; Cone gas flow rate: 150 L/h; Nebulizer pressure: 7 Bar.

Table 5
Mass spectrometry parameters of 8 fungal toxins.

Mycotoxins	Scan mode	Parent ion/(m/z)	Cone voltage/V	Daughter ion/(m/z)	Collision Energy/V
AFB1	ESI+	313.1	40	285[a]	21
				241	35
AFB2	ESI+	315.1	54	287[a]	25
				259	29
AFG1	ESI+	329.1	55	311	19
				243[a]	26
AFG2	ESI+	331.1	65	313	23
				245[a]	26
DON	ESI+	297.09	6	248.9[a]	10
				230.83	12
ZEM	ESI-	317.1	13	174.7[a]	−24
				130.5	−32
T-2 toxin	ESI+	489.3	25	387.2[a]	19
				245	27
AFM1	ESI+	329.1	52	273[a]	16
				258.9	24

[a] Quantitative Ion Pair.

2.3.8. UHPLC-QqQ-HRMS

This section has been published separately, so it is briefly described in this article (Fang et al., 2024). Liquid Chromatography Conditions: The ultra-performance liquid chromatography (UPLC) conditions were set as follows: ACQUITY UPLC® BEH C18 Column (1.7 μm, 2.1 × 100 mm); mobile phase A: 0.1 % formic acid aqueous solution; mobile phase B: acetonitrile; flow rate: 0.3 mL/min; column temperature: 40 °C; injection volume: 3 μL; gradient elution program as shown in Table 4. Mass Spectrometry Parameters for Eight Mycotoxins (See Table 5).

2.3.9. Data analysis

During the sequencing data processing stage, several quality control steps were performed on the obtained paired-end sequencing data. This included removing sequencing adapters and barcode sequences, followed by merging paired-end reads, and discarding sequences of poor quality and those that did not meet predetermined length standards. Chimeric sequences were also removed, with the percentage of chimeric sequences flagged and removed being below 10 %. Length filtering and denoising were performed using DADA2. After obtaining accurate ASV (Amplicon Sequence Variant) data, alpha diversity and beta diversity analyses were conducted. Additionally, species annotation was performed on the ASV sequences using the RDP and UNITE databases 2019 Version to identify microbial species in the samples. Finally, based on the ASV relative abundance table, detailed statistics were compiled on the relative relative abundance of each species in different samples.

Table 6
Content of fungal toxins from different regions (X±SD μg/kg).

source	DON	AFB2	AFG2	ZEN
GZXR	303.439 ± 14.185	–	–	129.767 ± 12.591
GZQL	80.676 ± 0.714	–	–	0.343 ± 0.107
YNFY	20.227 ± 1.053	0.464 ± 0.185	–	120.046 ± 6.837
YNQJ	11.003 ± 0.233	0.422 ± 0.058	0.029 ± 0.05	101.306 ± 9.686
GD	1.106 ± 0.133	–	–	–
LN	1.787 ± 0.066	–	–	–
GXBS	189.216 ± 3.62	–	–	5.203 ± 0.108
YNHH	76.562 ± 2.767	–	–	25.805 ± 2.119

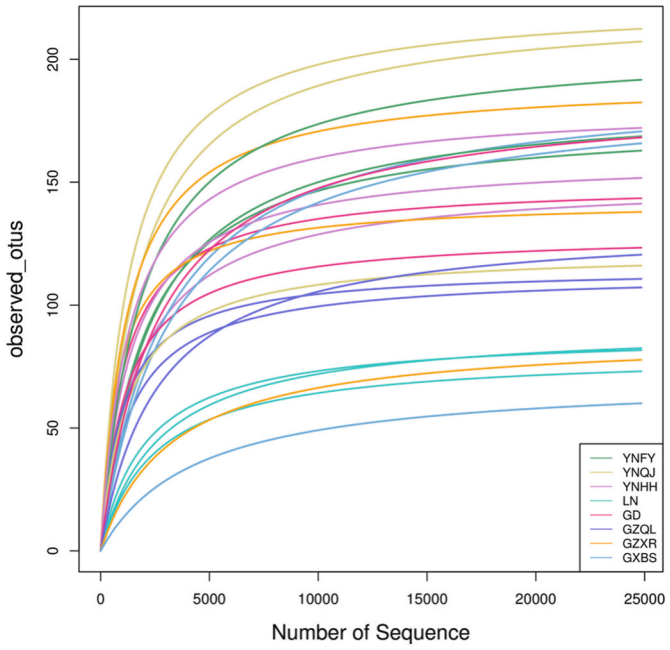

Fig. 1. Rarefaction curve.

3. Result

3.1. Fungal detection of Coix seed samples at different maturity stages

Fungal detection was conducted on *Coix* seed samples at various maturity stages, but no fungi were identified. Additionally, using the QuEChERS method combined with liquid chromatography-mass spectrometry established earlier in the study, it was determined that fungal toxins were absent. Therefore, it is hypothesized that a special mechanism or metabolic product developed during the *Coix* seed maturation process effectively inhibits fungal attachment and growth, thereby preventing the accumulation of fungal toxins.

3.2. The fungal toxin content of the selected sample

The samples of *Coix* seed were collected through preliminary experiments, and after testing, it was found that these samples contain high and low levels of mycotoxins. The collection area includes the main production area of *Coix* seed. The specific detection situation is shown in Table 6.

3.3. Comparison of microbial communities based on different origins

A total of 24 *Coix* seed samples from eight production areas were sequenced for 255 fungal content. Fig. 1 displays the rarefaction curve. After quality control, splicing, filtering, and DADA2 denoising, 1,872,393 valid sequences were obtained. Specific valid sequence

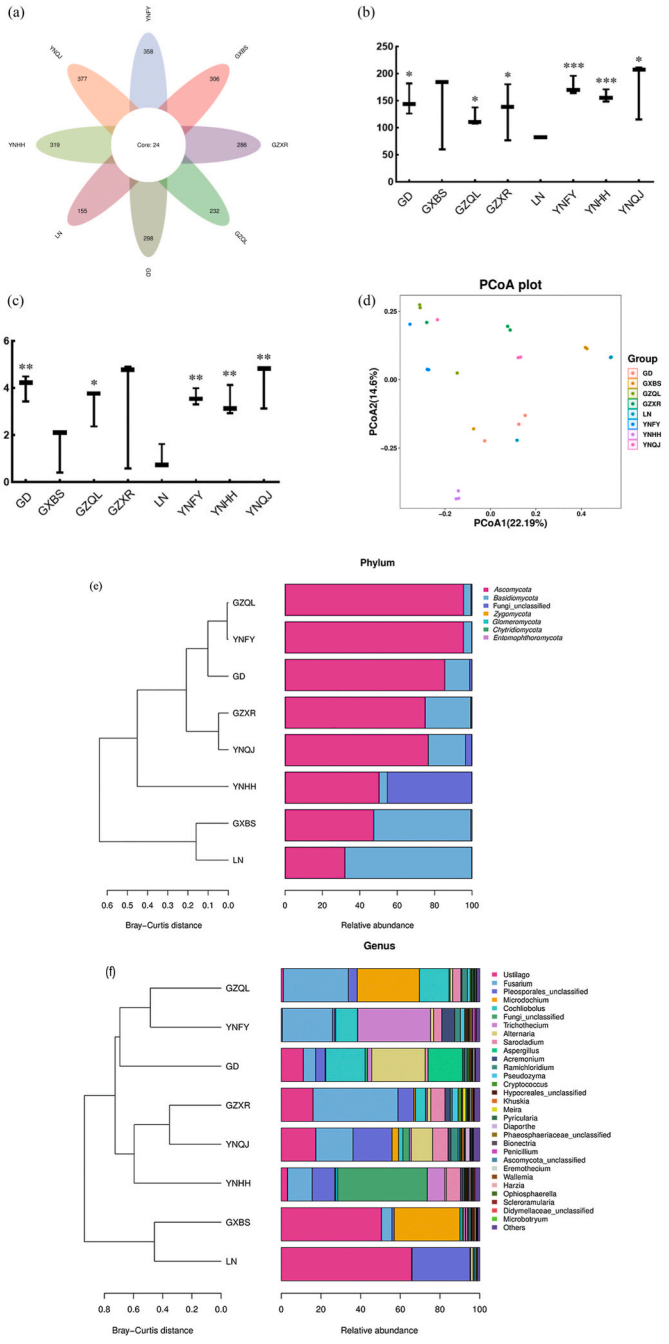

Fig. 2. Fungal distribution of *Coix* seed samples from different origins (a): Venn diagram. (b): Chao1 index. (c): Shannon index. (d): Principal coordinate analysis based on Bray Curtis distance matrix. (e): Fungal composition at the phylum level. (f): Fungal composition at the genus level. *P < 0.05, **P < 0.001, ***P < 0.001.

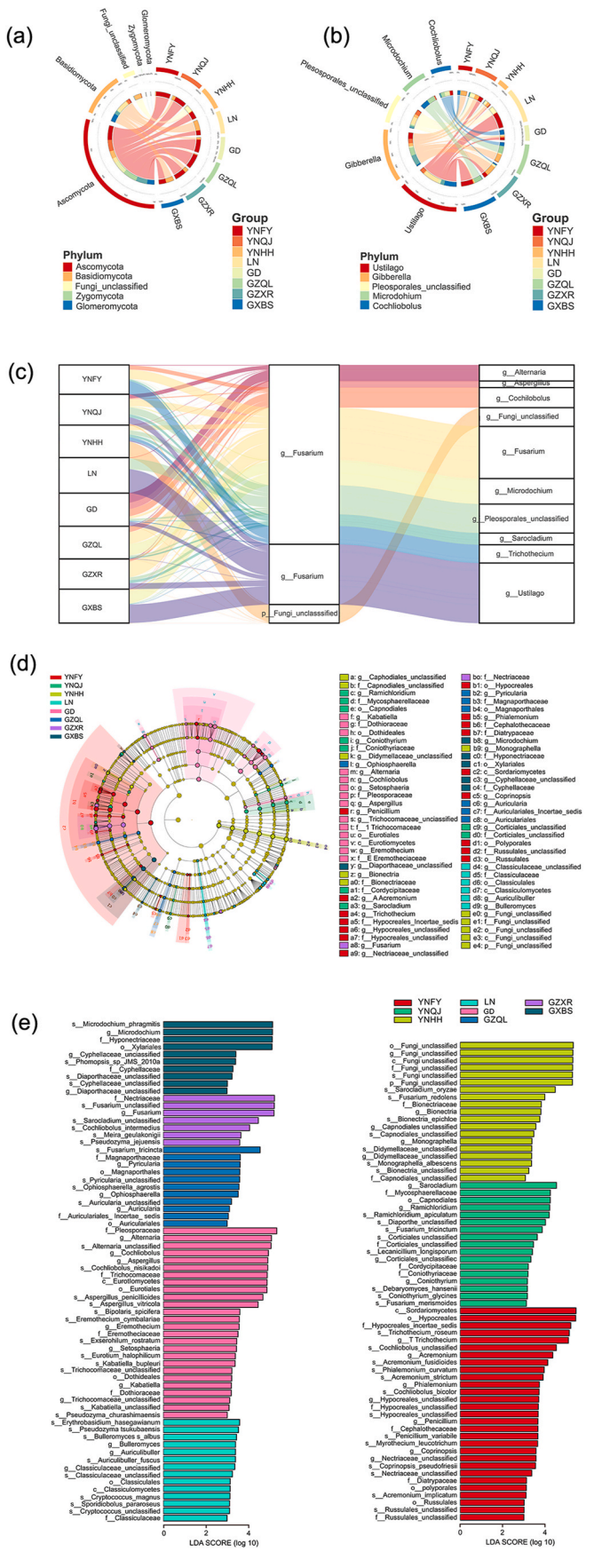

(caption on next column)

Fig. 3. (a): Abundance of the top 5 microbial communities at the phylum level. (b)Abundance of the top 5 microbial communities at the genus level. (c): Distribution of fungi from different regions, shown through mulberry plots at both the phylum and genus levels. (d) and (e): LEfSe (Linear discriminant analysis Effect Size) differential analysis highlighting significant differences among the microbial communities. This figure provides a comprehensive overview of the dominant microbial phyla and genera in *Coix* seed samples from various regions, along with detailed differential analyses.

counts for each region were as follows: 248,104 for YNFY, 255,157 for YNQJ, 252,412 for YNHH, 248,245 for LN, 244,744 for GD, 253,093 for GZQL, 245,025 for GZXR, and 241,584 for GXBS. The dilution curve showed stabilization with increasing sample size, indicating that the sequencing data approached saturation and could comprehensively reflect the sample biodiversity. Cluster analysis of ASVs from different regions was visualized with Venn plots, revealing 358, 306, 286, 232, 298, 155, 319, and 377 ASV feature sequences in YNFY, GXBS, GZXR, GZQL, GD, LN, YNHH, and YNQJ, respectively, with 24 common ASV feature sequences across all eight groups (Fig. 2a). The Chao1 and Shannon indices, commonly used in ecological research, were employed to assess fungal diversity. The Chao1 index quantifies species richness, while the Shannon index evaluates both richness and evenness. The LN samples exhibited a significantly lower Chao1 and Shannon index compared to GD, GZQL, YNFY, YNHH, and YNQJ samples, indicating lower fungal diversity consistent with fungal toxin content detection results (Fig. 2b and c).

Beta diversity analysis using Principal Coordinate Analysis (PCoA) based on the Bray-Curtis distance matrix illustrated clustering patterns. Closer distances between samples indicated similar microbial compositions, while greater distances reflected compositional differences. Notably, *Coix* seed samples from Yunnan displayed variations among YNFY, YNQJ, and YNHH, with differing fungal toxin content corresponding to microbial composition (Fig. 2d).

Further classification of ASVs revealed the following phyla: Ascomycota, Basidiomycota, Zygomycota, Glomeromycota, Chytridiomycota, and Entomophthoromycota. In GZQL, YNFYA, and GD, the Ascomycota phylum dominates, accounting for 94.78 %, 93.46 %, and 81.35 % of the community, respectively. In LN and GXBS, Basidiomycota dominates, accounting for 94.74 % and 77.57 % of the community, respectively. In YNHH and YNQJ, Fungi_unclassified dominates with 56.38 %, while Zygomycota, Glomeromycota, Chytridiomycota, and Entomophthoromycota contribute almost 0 % to the community in these eight regions (Fig. 2e). At the genus level, *Ustilago*, *Fusarium*, *Microrhizobium*, *Alternaria*, *Cochliobolus*, *Aspergillus*, and *Trichothecium* were the most prevalent, with these genera showing the highest potential for toxin production (Fig. 2f).

As shown in Fig. 3, a detailed genus-level analysis of *Coix* seed samples from eight different production areas revealed distinct enrichment patterns. In YNFY samples, *Fusarium* and *Trichothecium* were the predominant genera, with relative abundances of 25.36 % and 36.68 %, respectively. YNQJ samples were enriched in *Ustilago*, *Fusarium*, *Pleosporales*, *Alternaria*, and *Sarocladium*, with proportions of 17.45 %, 18.73 %, 19.66 %, 10.75 %, and 7.75 %, respectively. In YNHH samples, *Trichothecium*, *Sarocladium*, *Pleosporales*, and *Fusarium* were the main genera, representing 8.86 %, 7.07 %, 11.42 %, and 12.38 %, respectively.

LN samples exhibited high enrichment of *Ustilago*, *Pleosporales*, and *Alternaria*, accounting for 65.66 %, 29.17 %, and 1.19 %, respectively. GD samples were dominated by *Fusarium*, *Ustilago*, *Alternaria*, and *Aspergillus*, with respective relative abundances of 6.18 %, 11.09 %, 19.5 %, and 17.41 %. GZQL samples showed high levels of *Fusarium*, *Microdochium*, and *Cochliobolus*, with 32.77 %, 31.29 %, and 14.84 %, respectively. GZXR samples had prominent populations of *Fusarium*, *Ustilago*, *Pleosporales*, and *Sarocladium*, with rates of 42.86 %, 15.97 %, 8.03 %, and 7.12 %, respectively. GXBS samples were primarily composed of *Fusarium*, *Ustilago*, and *Microdochium*, with proportions of

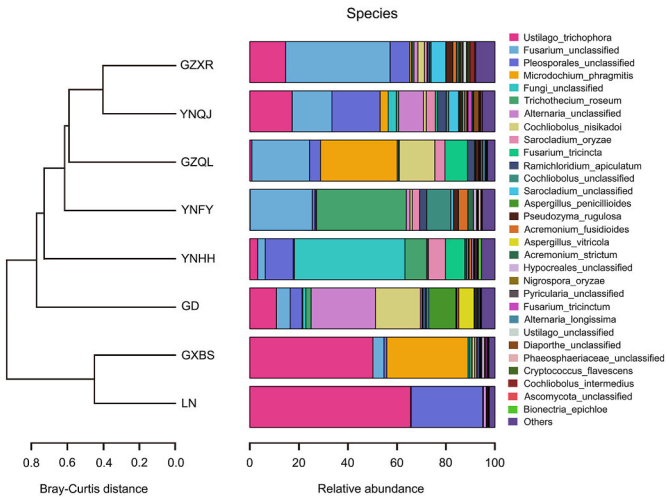

Fig. 4. Fungal composition at the species level.

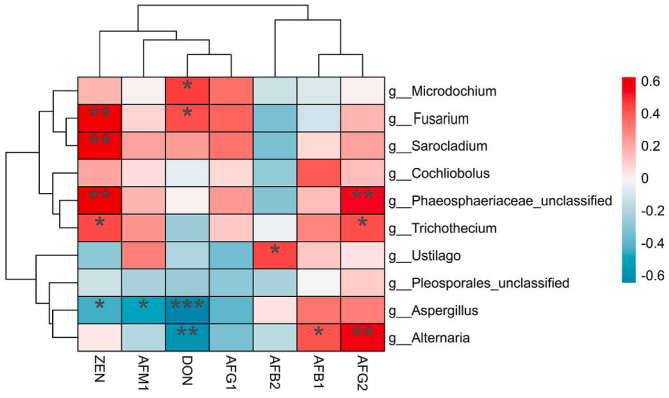

Fig. 5. The correlation analysis between fungi and fungal toxin content based on Spearman correlation analysis. *P < 0.05, **P < 0.001, ***P < 0.001.

5.26 %, 50.52 %, and 33.15 %, respectively. These findings indicate that the dominant fungal communities vary across different production areas, and their composition is closely associated with the production of fungal toxins.

At the species level, *Trichothecium roseum* was enriched in YNFY and YNHH samples, with concentrations of 36.65 % and 8.85 %, respectively. *Ustilago trichophora* was predominant in LN and GXBS samples, with concentrations of 65.61 % and 50.25 %, respectively. *Micropodium phragmitis* was found in GXBS and GZQL samples, with concentrations of 33.15 % and 31.29 %, respectively. *Aspergillus penicillioides* and *Aspergillus vitricola* were enriched in GD samples, with concentrations of 11.09 % and 6.24 %, respectively. *Fusarium tricinctum* was prevalent in YNQJ samples, accounting for 1.62 %. *Fusarium tricincta* was found in YNHH and GZQL samples, with concentrations of 7.92 % and 9.23 %, respectively. *Cochliobolus nisikadoi* was enriched in GD and GZQL samples, with concentrations of 18.26 % and 14.53 %, respectively. *Acremonium strictum* and *Acremonium fusidioides* were present in YNFY samples, with concentrations of 3.79 % and 2.28 %, respectively. Additionally, an unidentified strain within the genus *Fusarium* was detected in the samples, with concentrations ranging from 0.26 % to 42.63 %. These findings highlight the enrichment of genera such as *Ustilago*, *Trichothecium*, *Microdochium*, *Aspergillus*, *Fusarium*, *Fusarium*, and *Acremonium* (Fig. 4).

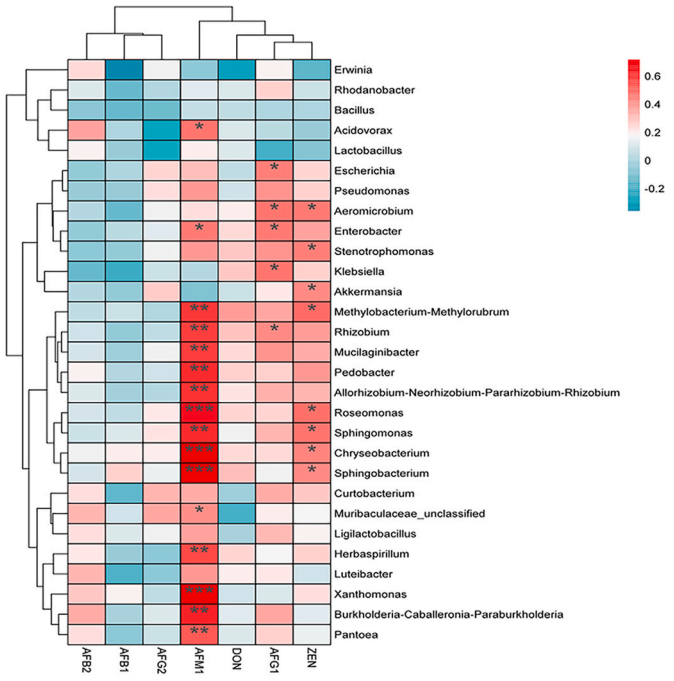

Fig. 6. Correlation analysis between bacteria and fungal toxin content based on Spearman correlation analysis *P < 0.05, **P < 0.001, ***P < 0.001.

3.4. Analysis of the association between fungal toxins and carrying fungi

A correlation analysis of the top 10 fungal genera based on fungal toxin content and relative abundance from different regions revealed significant correlations (*P < 0.05) between the content of zearalenone and the genera *Fusarium*, *Sarocladium*, *Pleosporales*, and *Trichothecium*. Significant correlations were also found between the content of deoxynivalenol and the genera *Fusarium* and *Microdochium*. Additionally, aflatoxins were significantly correlated with the genera *Pleosporales*, *Ustilago*, *Alternaria*, and *Trichothecium* (Fig. 5).

3.5. Correlation analysis between fungal toxins and carrying bacteria

Correlation analysis between fungal toxin content and carrying bacteria in *Coix* seed samples from different regions. The experiment found a negative correlation between *Bacillus* and all detected fungal toxins (Fig. 6).

3.6. The effect of antagonistic bacteria on the toxin production of *Aspergillus flavus*

The detection of aflatoxin revealed that no significant aflatoxin bulid-up was observed in the blank group, with the aflatoxin content being relatively low (Fig. 7). The control group exhibited significant growth of *Aspergillus flavus*, characterized by noticeable mycelium and yellow-green spore distribution on the surface of *Coix* seed samples. The detected aflatoxin content in the control group was significantly higher than in other groups. In contrast, the *Bacillus velezensis* and *Bacillus tequilensis* groups showed reduced surface distribution of *Aspergillus flavus* mycelium and spore growth, with aflatoxin content significantly lower than in the control group. Aflatoxins were mainly detected as AFB1 and AFB2, with aflatoxins G1, G2, and M1 not being detected. Among these aflatoxins, AFB1 exhibited the highest toxicity. Under appropriate temperature and moisture conditions, the toxin production of *Aspergillus flavus* was at least four times higher than in the antagonistic groups (Fig. 7a and b). *Bacillus velezensis* demonstrated a better inhibitory effect on aflatoxin production compared to *Bacillus tequilensis*. Observations of the two antagonistic bacteria inhibiting *Aspergillus flavus*

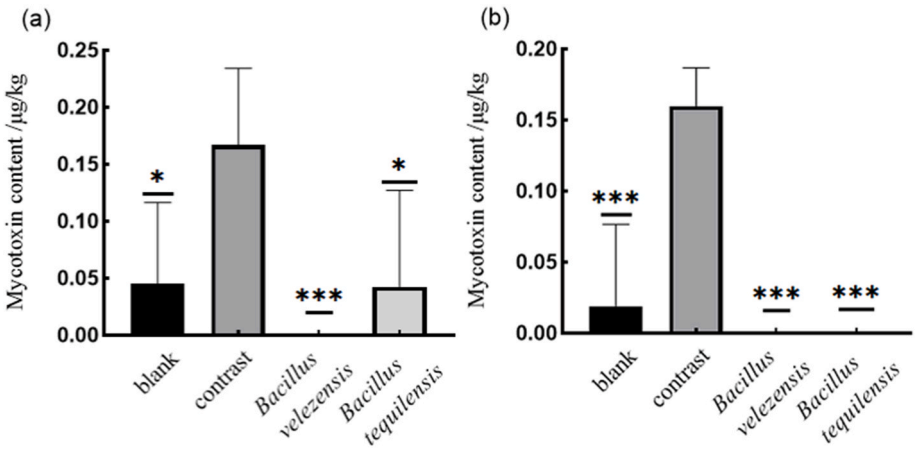

Fig. 7. (a): Detection level of aflatoxin B1. (b): Detection level of aflatoxin B2. *P < 0.05; ***P < 0.001.

growth and the subsequent analysis of fungal toxins showed that these antagonistic bacteria not only effectively inhibited *Aspergillus flavus* growth but also reduced its toxin production. This suggests that these antagonistic bacteria have potential as biocontrol agents for *Aspergillus flavus*, providing an effective method for controlling *Aspergillus flavus* contamination and inhibiting toxin production.

4. Discussion

In this study, high-throughput sequencing technology was employed to investigate the fungal communities present in *Coix* seed samples from various maturation stages and production regions(Li et al., 2024). The analysis revealed that *Coix* seeds, from the filling stage through to maturity, generally do not carry detectable levels of fungi, which is consistent with the observed low levels of fungal toxins in these seeds(Mi et al., 2017). However, fungi might have been detected in mature *Coix* seed samples from different regions, with variations in fungal diversity and abundance possibly reflecting regional differences and environmental influences, although this could only be speculated. As demonstrated in the study by Katati et al. (2023), weather conditions can alter fungal community composition, with distinct differences in the composition of fungal communities between low and high rainfall conditions.

The relative abundance of the dominant fungal phyla varied across different regions. In GZQL, YNFYA, and GD, the Ascomycota phylum dominated, accounting for 94.78 %, 93.46 %, and 81.35 % of the community, respectively. In contrast, in LN and GXBS, Basidiomycota was the predominant phylum, accounting for 94.74 % and 77.57 % of the community, respectively. In YNHH and YNQJ, the Fungi_unclassified group was dominant, making up 56.38 % of the fungal community. Additionally, the contributions of Zygomycota, Glomeromycota, Chytridiomycota, and Entomophthoromycota to the fungal communities in these eight regions were almost negligible based on the amplification and sequencing conditions. The Chao1 and Shannon indices indicated a significant reduction in fungal diversity and relative abundance in the LN group compared to samples from GD, GZQL, YNFY, YNHH, and YNQJ. This reduction in fungal diversity may be attributed to specific growth or storage conditions unique to the LN region, which could impact fungal community structure and composition.

Further analysis at the genus level identified several key fungal genera, including *Ustilago*, *Fusarium*, *Pleosporales*, *Alternaria*, *Trichothecium*, *Cochliobolus*, *Acremonium*, *Sarocladium*, *Aspergillus*, and *Microdochium*. Each genus exhibited varying levels of relative abundance across different regions. For instance, *Ustilago* and *Pleosporales* were most abundant in LN samples, with *Ustilago* reaching 65.66 % and *Pleosporales* 29.17 %. Conversely, *Trichothecium* was most prevalent in YNFY samples at 36.68 %, while *Sarocladium* was highest in YNQJ samples at 7.75 %. GD samples showed high relative abundances of *Alternaria* and *Aspergillus*, while *Cochliobolus* was most prevalent in GZQL samples. Notably, *Fusarium* reached its highest relative abundance in GZXR samples, and *Microdochium* was most abundant in GXBS samples.

Species-level analysis revealed dominant strains such as *Trichothecium roseum*, *Ustilago trichophora*, *Micropodium phragmitis*, *Aspergillus penicillioides*, *Aspergillus vitricola*, *Fusarium tricinctum*, *Fusarium tricincta*, *Cochliobolus nisikadoi*, *Acremonium strictum*, and *Acremonium fusidioides*. The correlation analysis between fungal genera and fungal toxins highlighted significant relationships: aflatoxins were strongly correlated with *Fusarium*, *Sarocladium*, *Pleosporales*, and *Trichothecium*; zearalenone and deoxynivalenol showed significant correlations with *Fusarium* and *Microdochium*; and aflatoxins were also correlated with *Pleosporales*, *Ustilago*, *Alternaria*, and *Trichothecium*. These findings align with previous studies identifying *Fusarium*, *Aspergillus*, and Alternaria as major contributors to fungal toxin accumulation (Rocha-Miranda and Venâncio, 2019; Su et al., 2018; Zheng et al., 2017). Additionally, *Trichothecium*, *Cochliobolus*, and *Acremonium* have been recognized as potential toxin producers (Jin An et al., 2016), whereas *Penicillium*, *Pyricularia*, and *Diaporthe* were not dominant in this study but remain potential toxin producers under certain conditions (Guo et al., 2020; Zhu et al., 2023).

The presence of *Ustilago trichophora*, a known pathogen causing black powdery mildew in *Coix* seeds, was predominantly observed in LN samples, indicating its role in crop damage and yield loss. The negative correlation observed between *Bacillus* species (*Bacillus velezensis* and *Bacillus tequilensis*) and fungal toxins suggests their potential as effective biocontrol agents(Lu et al., 2012, 2016). *Bacillus* strains not only inhibited *Aspergillus flavus* growth but also significantly reduced its toxin production, demonstrating their effectiveness in managing fungal contamination and toxin accumulation.

In interpretation, while *Coix* seeds generally show low levels of fungal toxins, the presence of potentially toxin-producing fungi poses a risk under favorable conditions for fungal growth. This study underscores the importance of effective antibacterial measures to control fungal contamination and toxin production. Implementing biocontrol strategies, such as using *Bacillus* strains, and improving storage and handling practices can enhance the safety and quality of *Coix* seeds, ensuring their suitability for consumption and medicinal use. Continued research and monitoring are essential to mitigate the risks associated with fungal contamination and ensure the safety of *Coix* seeds.

5. Conclusion

This study provides crucial insights into the fungal communities and toxin profiles in *Coix* seeds from various regions and maturation stages.

The results indicate that *Coix* seeds generally exhibit low levels of fungal contamination and toxin presence throughout maturation. Significant regional variations in fungal diversity were observed, with dominant genera including *Ustilago*, *Fusarium*, *Pleosporales*, *Alternaria*, *Trichothecium*, *Cochliobolus*, *Acremonium*, *Sarocladium*, *Aspergillus*, and *Microdochium*(Zhu et al., 2019). These genera are associated with fungal toxins, highlighting their potential impact on seed quality. Species-level analysis identified key strains such as *Trichothecium roseum*, *Ustilago trichophora*, *Micropodium phragmitis*, and others, with notable correlations to fungal toxins. *Bacillus* strains were found to effectively inhibit *Aspergillus flavus* and reduce aflatoxin production, suggesting their potential as biocontrol agents. Overall, the study underscores the need for effective fungal management strategies to ensure *Coix* seed safety. Enhanced storage practices and biocontrol measures could significantly improve seed quality and safety for consumption and medicinal use.

CRediT authorship contribution statement

Lingxia Peng: Conceptualization, Methodology, Data curation, Writing – original draft. **Jiahao Fang:** Investigation, Formal analysis, Data curation, Writing – original draft, LingxiaPeng and jiahaoFang contribute equally. **Lijun Yang:** Formal analysis, Software. **Gurusamy Abirami:** Translation. **Feng Yin:** Formal analysis, Software. **Lietao Cai:** Formal analysis, Software. **Chaojun Zhang:** Formal analysis, Project administration. **Yuyang Zhao:** Formal analysis. **Yan Jin:** Formal analysis. **Shuifeng Zhang:** Formal analysis. **Huadong Sheng:** Formal analysis. **Guohong Zeng:** Formal analysis. **Haimin Chen:** Formal analysis. **Zongsuo Liang:** Formal analysis. **Xiaodan Zhang:** Methodology, Supervision, Funding acquisition, Project administration.

Data availability

Data will be made available on request. The associated BioProject ID is PRJNA1188039.

Declaration of competing interest

The authors declare that they have no known competing financial interest or personal relationships that could have appeared to influence the work reported in this article.

Acknowledgements

This work was supported by the key project at central government level: The ability establishment of sustainable use for valuable Chinese medicine resources (2060302); The Major Science and Technology Projects of Breeding New Varieties of Agriculture in Zhejiang Province (No. 2021C02074). Zhejiang Sci-Tech University Excellent Postgraduate Dissertation Cultivation Fund (LW-YP2024069).

References

Arcella, D., Gergelova, P., Innocenti, M.L., Steinkellner, H., 2017. Human and animal dietary exposure to T-2 and HT-2 toxin. EFSA journal. European Food Safety Authority 15, e04972. https://doi.org/10.2903/j.efsa.2017.4972.

Chen, Amanda Juan, Jiao, Xiaolin, Hu, Yongjian, Lu, Xiaohong, Gao, Weiwei, 2015. Mycobiota and mycotoxins in traditional medicinal seeds from China. Toxins (10), 3858–3875. https://doi.org/10.3390/toxins7103858.

Chen, L., Li, Y., Yang, W., Li, B., Gou, Y., Zang, Z., Li Y& Wu, H., 2023. Exploring the Interventional Effect and Mechanism of *Coix* Seed Polysaccharides on Ulcerative Colitis in Vitro Inflammation Model Based on NLRP3/Caspase-1 Pathway, vol. 11. Journal of Chongqing Medical University, pp. 1323–1330. https://doi.org/10.13406/j.cnki.cyxb.003376.

Fang, Jiahao, Pan, Xiangjie, Yin, Fen, Zhang, Shuifeng, Gao, Tong, Feng, Tinghui, Chaojun, Zhao, Cai, Lietao, Liang, Zongsuo, Zhang, Xiaodan, 2024. Simultaneous determination of eight fungal toxins in *coix* seeds by QuEChERS ultra-high performance liquid chromatography tandem mass spectrometry[J/OL]. J. Zhejiang SCI-TECH Univ. 1–9. http://kns.cnki.net/kcms/detail/33.1338.TS.20241014.1056.040.html.

Guo, Mengyue, Jiang, Wenjun, Yu, Jingsheng, Yang, Meihua, Pang, Xiaohui, 2020. Research on the diversity of contaminated fungi in medicinal and edible *Coix* seed using high-throughput sequencing technology. World Chinese Medicine 15 (9), 1279–1284.

Han, X., Ji, X., Zhao, H., Zhang, Y., Liu, G., Wang, Y., Zhao, W., Wang, S., 2017. Mechanisma of *coix* seed compositions in the treatment of spleen deficiency and wet dampness Zheng. African journal of traditional, complementary, and alternative medicines AJTCAM 14, 239–246. https://doi.org/10.21010/ajtcam.v14i4.26.

Jiang, J., Li, X., Zhang, C., Wang, J& Li J., 2024. Anti-cancer effects of *Coix* seed extract through KCTD9-mediated ubiquitination of TOP2A in lung adenocarcinoma. Cell Div. (1). https://doi.org/10.1186/S13008-024-00112-2, 6-6.

Jin An, Tae, Seop Shin, Kyu, Chandra Paul, Narayan, Kim, Young Guk, Woo Cha, Seon, Moon, Yuseok, Oh, Seung Hun Yu&Sang-Keun, 2016. Prevalence, characterization, and mycotoxin production ability of Fusarium species on Korean adlay (*Coix lacrymal-jobi* L.) seeds. Toxins 8 (11), 310. https://doi.org/10.3390/toxins8110310.

Jin, Choi Hye, Tae-Jin, An, Juil, Kim, Park, Seong-Hwan, Kim, Dongwook, Young-Sup, Ahn, Yuseok, Moon, 2014. Postharvest strategies for deoxynivalenol and zearalenone reduction in stored adlay (*Coix lachryma-jobi* L.) grains. J. Food Protect. (3), 466–471. https://doi.org/10.4315/0362-028X.JFP-13-284.

Jin, K., Wang, F., Chen, L., Ge, Q., 2023. Separation, purification and antioxidant activity of *coix* seed polysaccharides. Cereals & Oils (12), 120–124.

Karlsson, I., Friberg, H., Steinberg, C., Persson, P., 2014. Fungicide effects on fungal community composition in the wheat phyllosphere. PLoS One 9, e111786.

Katati, B., Schoenmakers, P., Njapau, H., Kachapulula, P.W., Zwaan, B.J., van Diepeningen, A.D., Schoustra, S.E., 2023. Preharvest maize fungal microbiome and mycotoxin contamination: case of Zambia's different rainfall patterns. Appl. Environ. Microbiol. 89, e00078. https://doi.org/10.1128/aem.00078-23, 23.

Klindworth, A., Pruesse, E., Schweer, T., Peplies, J., Quast, C., Horn, M., Glöckner, F.O., 2013. Evaluation of general 16S ribosomal RNA gene PCR primers for classical and next-generation sequencing-based diversity studies. Nucleic Acids Res. 41, e1.

Li, H., Peng, L., Yin, F., Fang, J., Cai, L., Zhang, C., Xiang, Z., Zhao, Y., Zhang, S., Sheng, H., Wang, D., Zhang, X., Liang, Z., 2024. Research on Coix seed as a food and medicinal resource, it's chemical components and their pharmacological activities: a review. J. Ethnopharmacol. 319 (Pt 3), 117309. https://doi.org/10.1016/j.jep.2023.117309.

Liao, X., Li, Y., Long, N., Xu, Q., Li, P., Wang, J., Zhou, L., Kong, W., 2023. Multimycotoxin detection and human exposure risk assessment in medicinal foods. Food Res. Int. 164. https://doi.org/10.1016/J.FOODRES.2023.112456. Article 112456.

Lu, Y., Zhang, C., Zhao, H., Xing, X.H., 2012. Improvement of hydrogen productivity by introduction of NADH regeneration pathway in Clostridium paraputrificum. Appl. Biochem. Biotechnol. 167 (4), 732–742. https://doi.org/10.1007/s12010-012-9703-y.

Lu, Y., Zhao, H., Zhang, C., Xing, X.H., 2016. Insights into the global regulation of anaerobic metabolism for improved biohydrogen production. Bioresour. Technol. 200, 35–41. https://doi.org/10.1016/j.biortech.2015.10.007.

Mi, C., Yang, R., Rao, J., Yang, S., Wei, F., Li, O., Hu, X., 2017. Unveiling of dominant fungal pathogens associated with rusty root rot of panax notoginseng based on multiple methods. Plant Dis. 101 (12), 2046–2052. https://doi.org/10.1094/PDIS-01-17-0135-RE.

Miren, Castells, Ramos, Antonio J., Vicente, Sanchis, Marín, Sonia, 2007. Distribution of total aflatoxins in milled fractions of hulled rice. J. Agric. Food Chem. (7), 2760–2764. https://doi.org/10.1021/jf063252d.

Pfohl-Leszkowicz, Annie, Manderville, Richard A., 2007. Ochratoxin A: an overview on toxicity and carcinogenicity in animals and humans. Mol. Nutr. Food Res. (1), 61–99. https://doi.org/10.1002/mnfr.200600137.

Rocha-Miranda, F., Venâncio, A., 2019. Mycotoxigenic fungi in plant-based supplements and medicines. Curr. Opin. Food Sci. 3027–3031. https://doi.org/10.1016/j.cofs.2018.08.003.

Su, Chunyan, Hu, Yongjian, Gao, Dan, Yi, Luo, Chen, Amanda Juan, Weiwei, Jiao Xiaolin&Gao, 2018. Occurrence of toxigenic fungi and mycotoxins on root herbs from Chinese markets. J. Food Protect. 81 (5), 754–761. https://doi.org/10.4315/0362-028X.JFP-17-405.

Wang, J., Liu, L., Ball, T., Yu, L., Li, Y., Xing, F., 2016. Revealing a 5,000-y-old beer recipe in China. Proc. Natl. Acad. Sci. U. S. A 113, 6444–6448. https://doi.org/10.1073/pnas.1601465113.

Wu, Y., Ye, J., Xuan, Z., Li, L., Wang, H., Wang, S., Liu, H., Wang, S., 2021. Development and validation of a rapid and efficient method for simultaneous determination of mycotoxins in *Coix* seed using one-step extraction and UHPLC-HRMS. Food Addit. Contam. Part A, Chemistry, analysis, control, exposure & risk assessment 38, 148–159. https://doi.org/10.1080/19440049.2020.1833089.

Wu Y& Yuan, Y., 2010. Research progress on the chemical components and pharmacological activities of *Coix* seed. West China J. Pharm. Sci. (1), 111–113. https://doi.org/10.13375/j.cnki.wcjps.2010.01.019.

Zheng, Runsheng, Wang, Wenli, Tan, Jing, Hui, Xu, Zhan, Ruoting&Chen Weiwen, 2017. An investigation of fungal contamination on the surface of medicinal herbs in China. Chin. Med. 12 (1), 2. https://doi.org/10.1186/s13020-016-0124-7.

Zhu, B., Wang, S., Mi, C.Y., Yang, R.H., Zen, G.H., Hu, X.F., 2019. Genome sequence resource for ilyonectria mors-panacis, causing rusty root rot of panax notoginseng. Mol. Plant Microbe Interact. 32 (11), 1468–1471. https://doi.org/10.1094/MPMI-05-19-0118-A.

Zhu, Yaquan, Ma, Chunyan, Han, Xue, Piao, Chungen, Ning, Li Yong&Jiang, 2023. Two New Species of Diaporthe (Diaporthaceae, Diaporthales) in China. MycoKeys, pp. 95209–95228. https://doi.org/10.3897/MYCOKEYS.95.98969.